266

Long-Range Forecasting and Climate Research

Numerical simulation of seasonal Sahel rainfall in four past years using observed sea surface temperatures

by

J.A. Owen, C.K. Folland and M. Bottomley

LRFC 15

April 1988

LONG RANGE FORECASTING AND CLIMATE
RESEARCH MEMORANDUM NO 15

NUMERICAL SIMULATION OF SEASONAL SAHEL RAINFALL IN FOUR PAST YEARS USING OBSERVED SEA SURFACE TEMPERATURES

by

J A OWEN, C K FOLLAND AND M BOTTOMLEY

MET O 13 (SYNOPTIC CLIMATOLOGY BRANCH)
METEOROLOGICAL OFFICE
LONDON ROAD
BRACKNELL
BERKSHIRE RG12 2SZ

APRIL 1988

NUMERICAL SIMULATION OF SEASONAL SAHEL RAINFALL IN FOUR PAST YEARS USING OBSERVED SEA SURFACE TEMPERATURES

J. A. Owen, C. K. Folland and M. Bottomley
Meteorological Office, Bracknell, UK.

Abstract

Several general circulation model experiments have been carried out to investigate the influence of global sea surface temperatures (SSTs) on seasonal rainfall in the Sahel region of northern Africa, which has seen persistent drought in recent times. These experiments were run for 210 days each in "annual cycle" mode starting from identical initial atmospheric conditions for 26 March 1984. The experiments used interpolated monthly mean SSTs from April to October for four different years (1950, 1958, 1983 and 1984). The Sahel was extremely dry in two of these years (1983 and 1984), while it was much wetter than normal in 1958 and, especially, 1950.

These experiments showed a clear ability to simulate the large difference in rainfall between dry and wet years when the model was forced with the different SST patterns. They also showed large-scale changes in wind which were consistent with, but rather larger than, published observations of wind changes between less extreme Sahelian wet and dry periods.

In order to investigate the effects of soil moisture feedback in the model, some of the integrations allowed soil moisture to vary interactively while in others it followed (everywhere over the globe) the annual cycle of a soil moisture climatology. Soil moisture feedback amplified local differences between integrations, but had little effect on large-scale changes in atmospheric circulation.

The success of the simulations was judged sufficient to attempt hindcasts for the four years from July of each year to the end of October. The hindcasts were identical to the previous simulations except that after early July the SST anomalies were kept fixed, while the SST climatology, to which they were added, varied according to the season. These hindcasts produced results similar to the simulations in each year. This result tentatively indicates that GCMs may be used to supplement recently developed statistical techniques for forecasting seasonal Sahel rainfall, at least in the latter stages of such forecasts.

1. Introduction

The Sahel region of Northern Africa (see Fig. 1) has suffered from persistent drought in recent times (Dennett et al. 1985, Nicholson 1985). A time series of annual Sahel rainfall (which mostly falls between July and September) for this century (Fig. 2) shows that the rainfall has been below the long-term (1901-1980) mean in every year since 1968. By contrast, the 1950's had persistently above average rainfall.

Several mechanisms have been proposed to account for the persistence of dry conditions. Charney (1975) proposed a feedback mechanism involving the surface albedo. Reduced rainfall results in a lack of vegetation, which increases the albedo. As a consequence, there is net radiative cooling of the atmosphere, leading to subsidence and a further reduction in rainfall. That the albedo feedback could be important in principle has been demonstrated in general circulation models by Cunnington and Rowntree (1986) and Laval and Picon (1986). Evidence for real albedo changes is not conclusive (Norton et al. 1979, Courel et al. 1984).

Soil moisture is another factor: reduced local soil moisture content leads to reduced evaporation and less rainfall, thereby maintaining dry surface conditions. This was shown to be possible in a model by Walker and Rowntree (1977). Indeed, random changes in soil moisture over the Sahel could have similarly random positive feedback effects, enhancing rainfall in wet regions by increasing the moisture flux convergence from other regions and reducing rainfall in dry regions.

Anthropogenic effects must also be considered. While tropical deforestation is giving cause for concern (Henderson-Sellers and Gornitz 1984), the main problem in the Sahel region is the reduction of vegetation by overgrazing (Otterman 1977), causing a possible increase in the albedo and some reduction in soil water available for evaporation in and to the south of the Sahel.

This paper, while not ignoring the above local effects, is mainly concerned with changes in the general circulation of the atmosphere which may be associated with interannual variations in seasonal Sahel rainfall. It was originally thought that changes in the position of the Intertropical Convergence Zone (ITCZ) were responsible for such variations (Winstanley 1973). Lamb (1978) supported this theory with evidence that the equatorial pressure trough, the zone of maximum sea surface temperature and the axis of the subtropical high in the Atlantic were farther south than normal during Sub-Saharan dry years. The idea has been disputed (Miles and Folland 1974), and it was suggested instead (Nicholson 1981) that a "weakened intensity of the rainy season, independent of the ITCZ position" is the most common cause of drought in the Sahel, though variations in the latitude of the ITCZ were not ruled out. An analysis of West African rainfall for 1968-75 (Motha et al. 1980) did indicate a strong relationship between the position of the ITCZ and Sahel rainfall in most years, but years were also found in which rainfall was reduced over a wide range of West African tropical latitudes.

Newell and Kidson (1984) showed that, in relatively dry Sahel years, the low-level south-west winds that bring moisture into western North Africa were weaker and shallower in vertical extent than in relatively wet years, although they penetrated the usual distance inland. The same paper contains evidence of slightly reduced upper tropospheric easterly flow over the Sahel in dry years. Combined with weaker low-level westerly flow, this implies some reduction in vertical wind shear which might adversely influence the formation or intensity of easterly waves and squall lines (Hastenrath 1985) that are responsible for much of the rainfall in the Sahel (Riehl 1979). The frequency of squall lines appears to be lower in dry seasons, but the number of easterly waves has shown little variation from year to year (Hastenrath 1985, p.244).

2. Sea surface temperatures

Many general circulation model (GCM) experiments have demonstrated the existence of some effects of tropical sea surface temperature (SST) anomalies on the atmosphere (e.g. Palmer and Mansfield 1984, Shukla and Wallace 1983) and it has been shown that the inclusion of observed as opposed to climatological SSTs has a beneficial effect on the skill of some extended-range dynamical forecasts (Mansfield 1986, Owen and Palmer 1987).

A number of authors (e.g. Lamb 1978, Lough 1986, Hastenrath 1984) have suggested connections between Sahel rainfall and tropical Atlantic SSTs. Folland, Palmer and Parker (1986) showed for the first time, however, that persistently wet and dry periods in the Sahel are strongly related to SST anomalies on a near-global scale. They found a correlation coefficient between the Southern minus Northern hemisphere July to September SSTs (all of the Indian Ocean being included with the Southern hemisphere) and Sahel rainfall of -0.62 (significant at the 99.9% confidence level). The corresponding correlation obtained by using the Southern minus Northern Atlantic SSTs was only -0.44. Folland, Palmer and Parker (1986) also carried out GCM experiments which demonstrated strong effects of a composite SST anomaly (the difference in SST between five dry and five wet Sahel years) on Sahel rainfall. In further experiments, Palmer (1986) found quite strong individual effects from SST anomalies in the Atlantic, Pacific and Indian Oceans, but the largest effect was clearly from the global composite SST anomaly. Changes in the convergence of moisture into the Sahel were the most noticeable physical effect associated with the rainfall variations.

The aim of the present work was to model the effects of SSTs measured in individual wet (1950 and 1958) and dry (1983 and 1984) years. 1950 and 1984 were, respectively, the wettest and driest years in the Sahel this century (see Fig. 2). 1984 was interesting in that the ITCZ over the Atlantic was unusually far south in that year (Philander 1986). We should therefore be looking for evidence in the model results of both shifts in the latitude of the North African monsoon rainfall belt and changes in the large-scale tropical circulation.

We were also interested in assessing the importance of soil moisture feedback on our model results. We were able to do this since soil moisture content is a prognostic variable in our GCM, and we could include or exclude its variation.

3. Model and Experiments

All the experiments described here were carried out with the Meteorological Office 11-layer GCM (Slingo 1985), which has a resolution of 2.5° latitude by 3.75° longitude. Two versions of the model have been used to obtain the results in this paper. Most experiments used a model (model "3") much like that described by Cunnington and Rowntree (1986), with an interactive radiation scheme which assumes fixed, zonally averaged, climatological clouds (in July the percentage cover of convective cloud is taken to be 7% at 10°N and 4% at 20°N). The other experiments used an interactive radiation scheme which allows the prediction of changing cloud amounts from model variables (model "4"). Model 4 also incorporates a parametrization of orographic gravity wave drag (Palmer, Shutts and Swinbank 1986), improved calculations of soil temperature and some changes (increases) to surface albedo in the Sahara.

Both models have some deficiencies in their climate in the western Sahel. This is most noticeable in July and August when there is too little rainfall in the extreme west. This deficiency of rainfall is associated with excessively high surface air temperatures (especially daytime maximum temperatures), which may be caused by problems associated with the diurnal cycle. The errors in the climatology of model 4 are considerably larger than those of model 3, and it is likely that model 4 predicts too little cloud in the extreme western Sahel. In September, however, the rainfall and temperature climatologies of both models are good in this region. Overall, model 3 has decidedly the better climatology. Experience with dynamical long-range forecasting indicates strongly that unless a model has a reasonably good climatology for the region under consideration, then its response to perturbations to that regional climate will not be realistic. Therefore we feel justified in concentrating our attention on model 3 whose rainfall climatology is in reasonable accord with published climatologies (e.g. Todorov,1985), except in the far west Sahel early in the rainfall season.

Each experiment consisted of a 210-day integration in annual cycle mode, starting from the atmospheric conditions of 26 March 1984. The model uses "months" of 30 days each, so the seven "months" of each integration correspond approximately to April, May, ... , October. This approximation will be used throughout this paper. The first two months were intended to allow the model to adjust to the imposed SSTs from the identical starting conditions.

The SSTs used here were obtained as monthly means from the Meteorological Office Historical Sea Surface Temperature data set and interpolated to five-day means. However, this data set lacks observed values over an appreciable fraction of the globe and it is also necessary to provide continuity between the SST data and the ice edge. The appendix describes the techniques used for overcoming these problems. The integrations used SSTs from 1950, 1958, 1983 or 1984, updated every five days during the course of each integration. The average difference in SST between 1984 and 1950 for July to September is shown in Fig. 3. The corresponding difference between 1983 and 1958 SSTs is similar.

Soil moisture feedback in the model takes place through the interaction of the soil moisture content with precipitation, evaporation, runoff and snowmelt. Those experiments in which this interaction is allowed are labelled "(I)", and those in which the soil moisture takes climatological values (see section 5) are labelled "(C)". Unless otherwise stated, the results presented will be for model 3.

4. Results of experiments including soil moisture feedback

(a) Rainfall and soil moisture content

Figure 4 shows the modelled rainfall over north Africa for August from experiment 1950(I). The observed rainfall for August 1950, obtained from CLIMAT reports, is shown in Fig. 5. Apart from the details of the precipitation pattern in the coastal regions near the Gulf of Guinea and excessive rainfall in some parts of the central Sahara (where the climatology appears to be too wet), the simulation is remarkably good both as regards the pattern and amount of rainfall. The same is true of the July and September simulations though the July rainfall is generally underestimated, especially in the westernmost Sahel, and the September rainfall overestimated.

Figure 6 shows the corresponding rainfall from experiment 1984(I), and the observed rainfall for August 1984 is shown in Fig. 7. Again there is excess modelled rainfall over parts of the Sahara, especially in the mountainous Ahaggar region (4° to 10°E, 22° to 26°N), but generally the amounts are realistic.

Of particular interest is the difference in modelled rainfall between 1984(I) and 1950(I). This is shown as an average for July to September in Fig. 8, with the corresponding observed differences shown in Fig. 9. The differences in modelled rainfall are surprisingly realistic: the substantially reduced rainfall over the Sahel and the marked increase farther south are both shown. These results are consistent with the observation (Philander 1986) that the ITCZ was farther south than usual over the Atlantic in 1984.

As a result of these rainfall differences, which persist throughout the Sahel rainfall season, modelled soil moisture has, by September, become much larger in 1950 than in 1984 over the whole Sahel (Fig. 10).

The experiments with observed 1983 and 1958 SSTs gave similar results. The difference in rainfall between 1983(I) and 1958(I) is shown in Fig. 11. This figure is very similar to Fig. 8, both as regards the pattern and magnitude of the differences.

The difference in rainfall between 1984(I) and 1950(I) that was obtained using model 4 (corresponding to Fig. 8 for model 3) is shown in Fig. 12. Similarities between Figs. 12 and 8 are evident, especially over the oceans, where there is generally reduced rainfall near latitude 15° N, and increased rainfall to the south of this latitude. Over Africa, reduced rainfall over the eastern Sahel is clearly seen, but is not present over the western Sahel. One indirect reason for this is that model 4 has a considerably poorer rainfall climatology over the western Sahel than model 3, with too little rain. The lack of a substantial difference between experiments 1984(I) and 1950(I) with model 4 is a consequence of this failing and underlines the need for a model with a good regional climatology.

(b) Winds

Figure 13 shows the average 950mb wind climatology of model 3 for July to September. The cross-equatorial flow over the Atlantic and south-westerly monsoon flow into western North Africa are clearly seen. This flow is the primary source of moisture for the western Sahel region, so that any substantial change of this flow should have a major impact on Sahel rainfall.

Figure 14 shows the difference in 950mb wind between 1984(I) and 1950(I) for July to September. Over western North Africa this is in the opposite direction to the climatological wind, so the monsoon flow is weaker with the 1984 SSTs than with the 1950 SSTs. The corresponding difference for 250mb wind is shown in Fig. 15. This is in a westerly sense over most of the tropics and indicates a reduction of the normal upper-level easterly flow. These results are consistent with those of Newell and Kidson (1984), although their analysis did not include the extreme years 1950 and 1984. The differences between 1983(I) and 1958(I) are generally similar to those for 1984(I) and 1950(I), though slightly weaker.

The experiments using model 4 gave similar results. In order to investigate the statistical significance of these wind changes for 1950 and 1984, the results from models 3 and 4 were combined for the months of July to October, thus providing eight months for each of 1984(I) and 1950(I). A cross-section (an average over longitudes 10°W to 30°E) of the zonal wind difference between 1984(I) and 1950(I) is shown in Fig. 16. The zonal winds for each modelled month were converted into anomalies by subtracting the appropriate model climatology and these anomalies were used to calculate the student's t-statistic for the difference between 1984(I) and 1950(I). Regions where the magnitude of the t-statistic is greater than 2.1 are stippled in Fig. 16. On the assumption that the eight monthly mean anomalies (July to October) for each year are independent, the difference between 1984(I) and 1950(I) is significant at the

95% confidence level in these regions. However, the eight anomalies for each year are not truly independent, so the significance of the zonal wind changes has been overestimated. Figure 17 shows a similar calculation for the difference between 1983(I) and 1958(I) using only the results from model 3. This also shows a reduction in upper-level easterlies and lower-level westerlies in the dry year.

Figure 18 is the corresponding diagram for the global mean zonal wind difference, except that the winds for the two dry years have been combined as have the winds for the two wet years. It shows that the reduction in upper-level easterlies with the 1983 and 1984 SSTs is significant over the tropics as a whole and not just over North Africa.

5. Soil moisture feedback

Soil moisture feedback has been mentioned as a potentially important effect. The experiments of the previous section which used model 3 were re-run with the soil moisture everywhere over the land prescribed to follow the soil moisture climatology of model 3. This gave four further experiments in which soil moisture feedback could not take place.

Figure 19 shows time series of modelled rainfall for the whole Sahel for eight experiments (with interactive or climatological soil moisture), together with the observed rainfall for each of the four years. The ability of the model to simulate the different rainfall in each year is very encouraging, and this ability is present even when soil moisture feedback is prevented from taking place. However, this feedback mechanism does have an impact on the results. This is clearly seen in 1950 when the simulated soil moisture was very high and in 1983 when the simulated soil moisture was very low (Figure 20 shows time series of modelled soil moisture for the whole Sahel together with the climatology of model 3).

The effects of soil moisture feedback on the large-scale atmospheric response (e.g. changes in wind) are slight. Figure 21 shows the zonal wind difference, averaged between 10°W and 30°E, between 1984(C) and 1950(C) (climatological soil moisture). This is very similar to Fig. 16 which was based on experiments with interactive soil moisture (but also included results from model 4).

The effects on temperature are shown in Figs. 22 and 23 for a more limited latitude band. The large difference in temperature over the Sahel is present only in the experiments with interactive soil moisture. Clearly, soil moisture feedback strongly affects the local response to SST changes, but has relatively little effect on the large-scale changes in general circulation.

6. Hindcast Experiments

The results of the above experiments were sufficiently promising that it was decided to carry out experiments to test whether useful forecasts of Sahel rainfall might be possible. In this case there would be no prior knowledge of how the SST anomalies would change through the season. The experiments carried out were "hindcasts" in which it was attempted to simulate the rainfall for July to October in each of the four years given only a knowledge of the July SSTs. In practice, the SST anomalies for the pentad 11-15 July were added to the SST climatology for each pentad until the end of October, thus producing a forecast of the July to October SSTs based on persistence of the SST anomalies. These SSTs were then used in four hindcast experiments, each of which was otherwise identical to the corresponding experiment with observed SSTs.

Figure 24 shows time series of modelled Sahel rainfall for the experiments with observed SSTs and the hindcasts with fixed SST anomalies. In each case, interactive soil moisture was used. The hindcasts in general gave a similar amount of rainfall to the corresponding experiments in which the observed SSTs were used. A more stringent test would be to attempt to simulate the rainfall for the whole season given the SST anomalies in, say, May.

The hindcast experiments described above used persistence of SST anomalies as a forecasts of SST variations in each year. It might be possible to produce better SST forecasts using similar empirical techniques to those currently used in forecasting Sahel rainfall (Parker et al., 1988). It is hoped to test these ideas in the near future.

7. Conclusions

The Meteorological Office 11-layer model has shown a clear ability to simulate not only the observed rainfall climatology of the Sahel but, more importantly, observed changes in Sahel rainfall in response to changes in worldwide sea surface temperature. A calculation of the correlation between the monthly mean observed and simulated Sahel rainfall over all four years gave a value of 0.78.

Both versions of the model gave statistically significant changes in wind in response to the changed SSTs, and these changes are consistent with observed wind changes between wet and dry periods in the Sahel. Soil moisture feedback in the model amplified local differences between integrations, but the SSTs are mainly responsible for the large-scale atmospheric circulation changes which are thought to influence Sahel rainfall. Hindcast experiments were able to simulate July to October rainfall given only the July SSTs.

These results raise the question of the precise mechanisms by which the large-scale SST anomalies affect the large-scale circulation of the atmosphere which in turn modulates Sahel rainfall by more than one mechanism. This may be a difficult question to answer if, as seems likely from the work of Palmer (1986), different parts of the global ocean affect regional circulation over the Sahel in different ways. It is of especial interest to isolate the individual contributions of different oceanic regions. To start to tackle this problem, a new set of experiments has been designed, using model 3, to investigate the effects of the observed (a) tropical Atlantic , (b) global tropical and (c) global extratropical SST anomalies in the above four contrasting years. The results will be reported in a future note.

Appendix

A method of producing globally complete sea surface temperature (SST) fields for use in dynamical model experiments has recently been developed. To date, global monthly mean 5°×5° SST fields, based on the Met. Office Historical SST (MOHSST) dataset (Parker, 1987; Bottomley et al., 1988), and with climatological ice limits (Alexander and Mobley, 1976), have been created for the four years 1950, 1958, 1983 and 1984. The fields for 1950 and 1984 were created using an early version of the method, while those for 1958 and 1983 were created using the current version.

The basic MOHSST monthly fields contain significant areas of sparse data coverage, particularly in the Southern Ocean and the South Pacific Ocean. To make the fields spatially complete, information from the (global) 5°×5° SST climatology for 1951-80 (Bottomley et al., 1988) is blended into the missing data areas. Essentially the spatial rates of change of gradient in the missing data areas are set equal to those in the climatology, but the absolute values of the SSTs are related to the surrounding MOHSST data (where available). This is achieved by solving, subject to boundary conditions imposed by the MOHSST data, the following Poisson equation:

$$\nabla^2 \phi = \nabla^2 C \qquad \text{Eqn 1}$$

where C is the 1951-80 climatology, and   is the resulting blended SST field.

In the original method missing data areas were identified individually and the solution in each area obtained by reposing Eqn 1 as:

$$\nabla^2 (\phi - C) = 0 \qquad \text{Eqn 2}$$

The solution of this (Laplace's) equation was found by an integral equation method based on Green's formula (Symm and Pitfield, 1974). The solution was then added to the climatological values for each grid square. At, for example, the polarmost limits of areas such as the Southern Ocean, where there are no MOHSST data, boundary values were taken directly from the climatology.

This method was rather laborious as identification of missing data areas was done by eye. Also, isolated MOHSST data which could not be accommodated either on, or within, the boundaries of the MOHSST data had to be ignored.

In the current method, Eqn 1 (in spherical coordinates) is solved globally using a sequential relaxation procedure (see, for example, Thompson, 1961). Here the climatological ice limits provide the external boundary conditions for the solution (ice point temperatures are set equal to -1.8°C) and all the MOHSST data are retained as internal boundary conditions. These boundary values are kept fixed but at missing data points (i,j) Eqn 1 is solved iteratively with the climatology supplying the "initial guess" values, i.e. $\phi^{0}_{ij} = C_{ij}$. Successive values of ϕ_{ij} are then evaluated according to:

$$\phi^{m+1}_{ij} = \phi^{m}_{ij} + \alpha R^{m}_{ij}$$

where R^{m}_{ij} , the residual at the mth iteration step,

$$= \phi^{m}_{i+1,j} + \phi^{m}_{i,j+1} + \phi^{m+1}_{i-1,j} + \phi^{m+1}_{i,j-1} - 4\phi^{m}_{ij} - F_{ij}$$

(for simplicity, spherical coordinates have not been used here)

$$F_{ij} = \nabla^2 C_{ij}$$

m is the iteration step,

and α is the coefficient of relaxation (α=1.6).

The iteration is continued until $R^{m}_{ij} < \epsilon$ for all R^{m}_{ij} , where ϵ=0.0001. This method is based on that used at the Climate Analysis Center, Washington, in their blended SST analysis (Reynolds, 1987) and substantially reduces both the human effort and the computer time involved compared with our original system.

References

R. C. Alexander and R. L. Mobley, 1976, Monthly average sea-surface temperatures and ice-pack limits on a 1° global grid. *Mon. Wea. Rev.*, **107**, 896-910.

M. Bottomley, C. K. Folland, J. Hsiung, R. E. Newell and D. E. Parker, 1988, *Global Ocean Surface Temperature Atlas (GOSTA)*, A Joint Project of the Meteorological Office and the Massachusets Institute of Technology (in press).

J. G. Charney, 1975, Dynamics of deserts and drought in the Sahel. *Quart. J. R. Met. Soc.*, **101**, 193.

M. F. Courel, R. S. Kandel and S. I. Rasool, 1984, Surface albedo and the Sahel drought. *Nature*, **307**, 528-531.

W. M. Cunnington and P. R. Rowntree, 1986, Simulations of the Saharan atmosphere - dependence on moisture and albedo. *Quart. J. R. Met. Soc.*, **112**, 971-999

M. D. Dennett, J. Elston and J. A. Rodgers, 1985, A reappraisal of rainfall trends in the Sahel. *J. Climatology*, **5**, 353-361.

C. K. Folland, T. N. Palmer and D. E. Parker, 1986, Sahel rainfall and worldwide sea temperatures, 1901-85. *Nature*, **320**, 602-607.

S. Hastenrath, 1984, Interannual variablility and annual cycle: mechanisms of circulation and climate in the tropical Atlantic sector. *Mon. Wea. Rev.*, **112**, 1097-1107.

S. Hastenrath, 1985, *Climate and circulation of the tropics*. D. Reidel, Dordrecht, 445 pp.

A. Henderson-Sellers and V. Gornitz, 1984, Possible climatic impacts of land cover transformations, with particular emphasis on tropical deforestation. *Climatic change*, **6**, 231-257.

P. J. Lamb, 1978, Large scale tropical Atlantic surface circulation patterns associated with sub-Saharan weather anomalies. *Tellus*, **30**, 240-251.

K. Laval and L. Picon, 1986, Effect of a change of surface albedo of the Sahel on climate. *J. Atmos. Sc.*, **43**, 2418-2429

J. M. Lough, 1986, Tropical Atlantic Sea Surface Temperatures and Rainfall variations in Subsaharan Africa. *Mon. Wea. Rev.*, **114**, 561-570.

D. A. Mansfield, 1986, The skill of dynamical long-range forecasts, including the effect of sea surface temperature anomalies. *Quart. J. R. Met. Soc.*, **112**, 1145-1176.

M. K. Miles and C. K. Folland, 1974, Changes in the latitude of the climatic zones of the Northern Hemisphere. *Nature*, **252**, 616.

R. P. Motha, S. K. Leduc, L. T. Steyaert, C. M. Sakamoto and N. D. Strommen, 1980, Precipitation patterns in West Africa. *Mon. Wea. Rev.*, **108**, 1567-1578.

R. E. Newell and J. W. Kidson, 1984, African mean wind changes between Sahelian wet and dry periods. *J. Climatology*, **4**, 27-33.

S. E. Nicholson, 1981, Rainfall and Atmospheric Circulation during Drought Periods and Wetter Years in West Africa. *Mon. Wea. Rev.*, **109**, 2191-2209.

S. E. Nicholson, 1985, Sub-Saharan rainfall 1981-84. *J. Clim. Appl. Met.*, **24**, 1388-1391.

C. C. Norton, F. R. Mosher and B. Hinton, 1979, An investigation of surface albedo variations during the recent Sahel drought. *J. Appl. Met.*, **18**, 1252-1262

J. Otterman, 1977, Anthropogenic Impact on the Albedo of the Earth. *Climatic Change*, **1**, 137-155.

J. A. Owen and T. N. Palmer, 1987, The impact of El Niño on an ensemble of extended-range forecasts. *Mon. Wea. Rev.*, **115**, 2103-2117.

T. N. Palmer and D. A. Mansfield, 1984, The response of two atmospheric general circulation models to sea surface temperature anomalies in the tropical east and west Pacific. *Nature*, **310**, 483-485.

T. N. Palmer, 1986, Influence of the Atlantic, Pacific and Indian Oceans on Sahel Rainfall. *Nature*, **322**, 251-253.

T. N. Palmer, G. Shutts and R. Swinbank, 1986, Alleviation of a systematic westerly bias in general circulation and numerical weather prediction models through an orographic gravity wave drag parametrization. *Quart. J. R. Met. Soc.*, **112**, 1001-1040.
D. E. Parker, 1987, The Meteorological Office Historical Sea Surface Temperature Data Set, *Meteorol. Mag.*, **116**, 250-254.
D. E. Parker, C. K. Folland and M. N. Ward, 1988, Sea surface temperature anomaly patterns and prediction of seasonal rainfall in the Sahel region of Africa. *Recent climatic change - a regional approach* (ed. S. Gregory), Belhaven Press (in press).
S. G. H. Philander, 1986, Unusual conditions in the tropical Atlantic Ocean in 1984. *Nature*, **322**, 236-238.
R. W. Reynolds, 1988, A real-time global sea surface temperature analysis. *J. Climate*, **1**, (in press).
H. Riehl, 1979, *Climate and weather in the tropics*, Academic Press.
J. Shukla and J. M. Wallace, 1983, Numerical simulation of the atmospheric response to equatorial Pacific sea surface temperature anomalies. *J. Atmos. Sci.*, **40**, 1613-1630.
A. Slingo, 1985, Handbook of the Meteorological Office 11-layer atmospheric general circulation model. *Dynamical Climatology Technical Note No. 29*, Meteorological Office, Bracknell.
G. T. Symm and R. A. Pitfield, 1974, Solution of Laplace's equation in two dimensions. *NPL Report NAC 44*.
P. D. Thompson, 1961, *Numerical Weather Analysis and Prediction*, Macmillan and Co.
A. V. Todorov, 1985, Sahel: The Changing Rainfall Regime and the "Normals" Used for its Assessment. *J. Clim. Appl. Met.*, **24**, 97-107.
J. Walker and P. R. Rowntree, 1977, The effect of soil moisture on circulation and rainfall in a tropical model. *Quart. J. R. Met. Soc.*, **103**, 29-46.
D. Winstanley, 1973, Recent rainfall trends in Africa, the Middle East and India. *Nature*, **243**, 464-465.

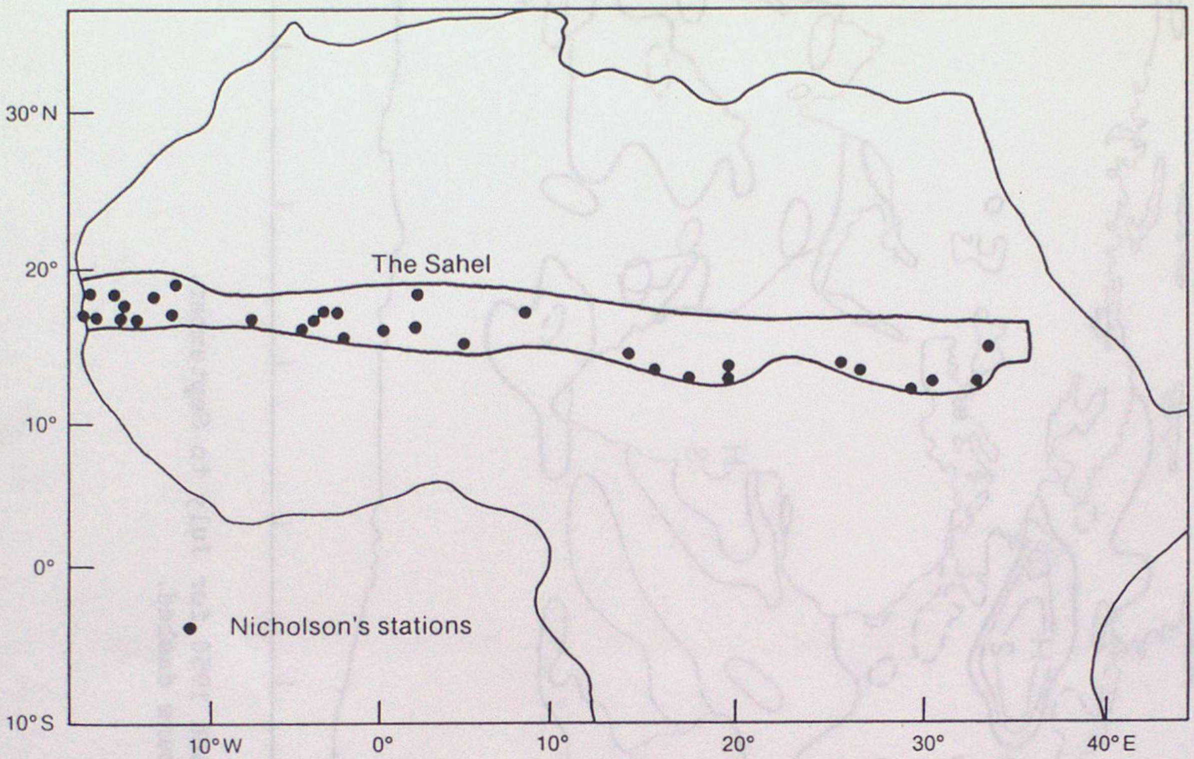

Figure 1 The Sahel region as defined by Nicholson (1985)

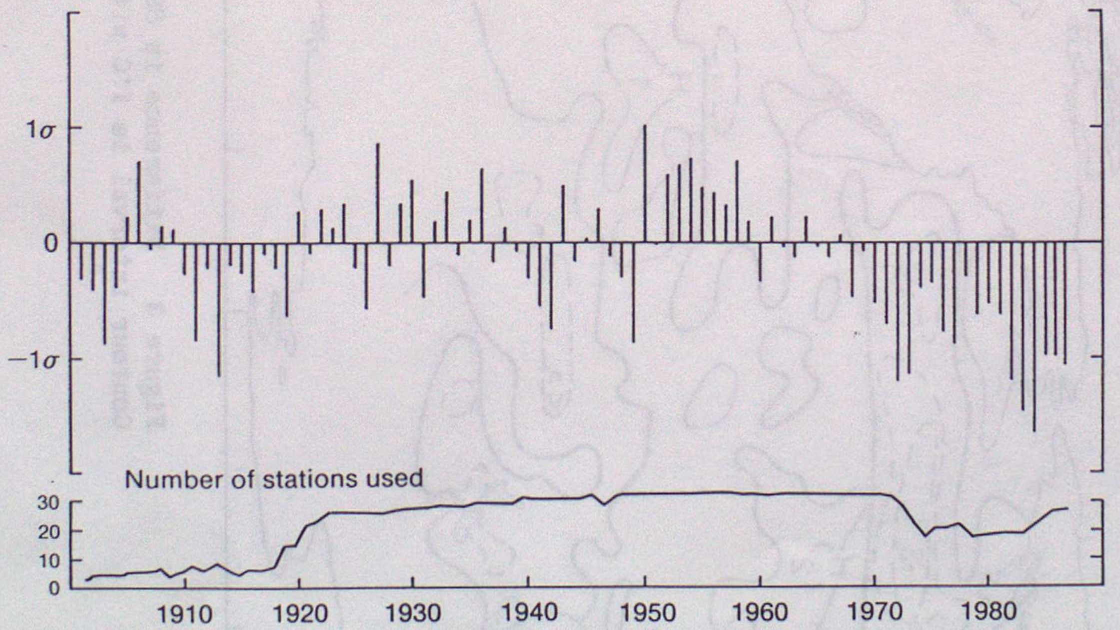

Figure 2 Standardized annual rainfall anomalies for the Sahel, 1901-1987 (upper panel). Values to 1984 are after Nicholson (1985); 1985-1987 values are from CLIMAT reports. The lower panel gives the number of stations used.

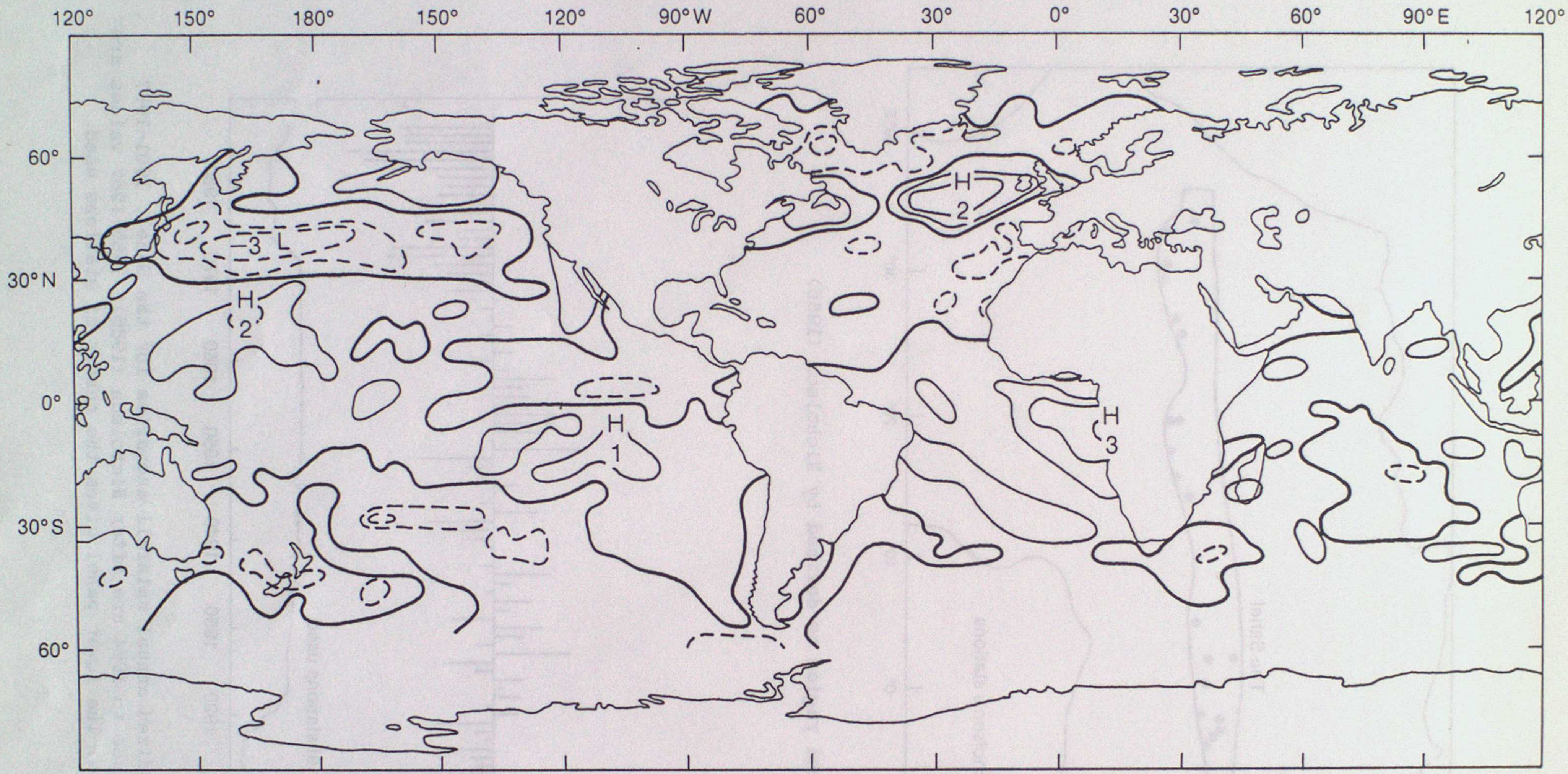

Figure 3 Difference in SST between 1984 and 1950 for July to September.
Contour interval is 1°C with negative contours dashed.

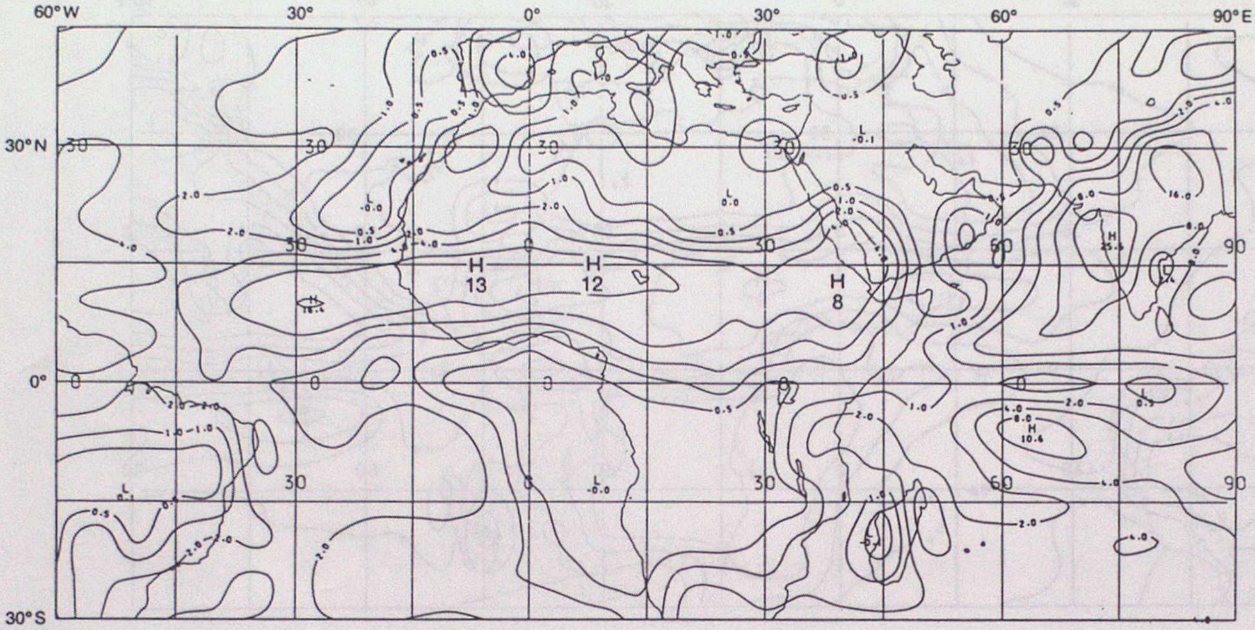

Figure 4 Modelled August rainfall for experiment 1950(I). Contours are at 0.5, 1, 2, 4, 8 and 16 mm day⁻¹.

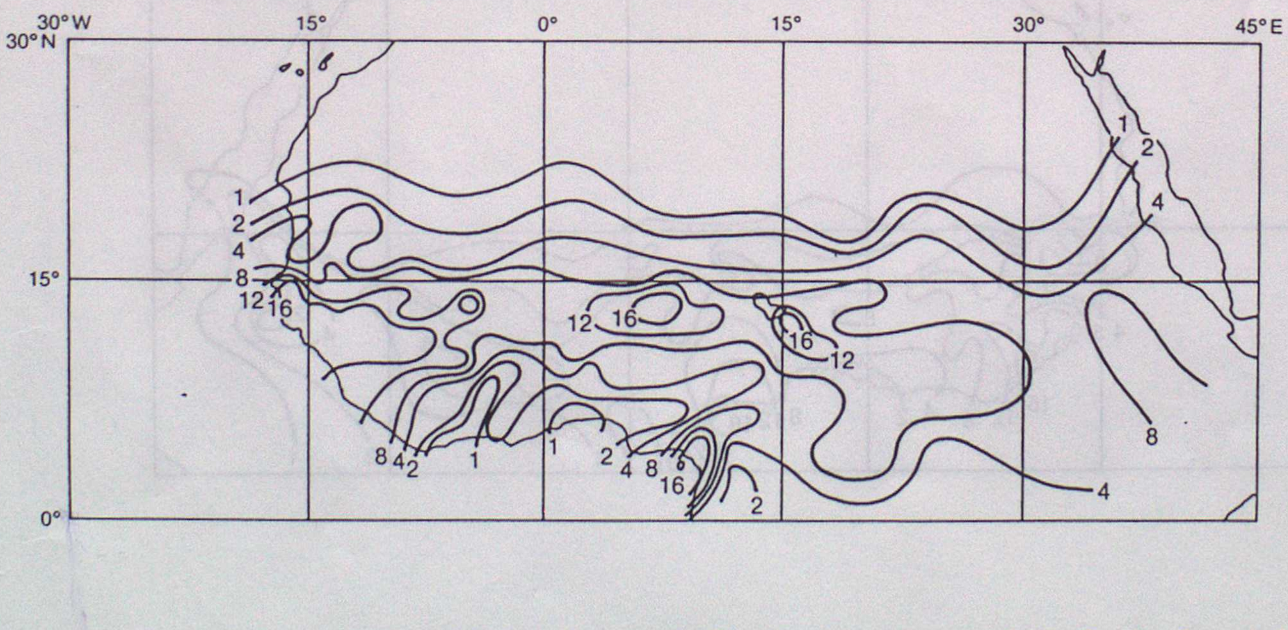

Figure 5 Observed rainfall for August 1950. Contours are at 1, 2, 4, 8 and 16 mm day⁻¹.

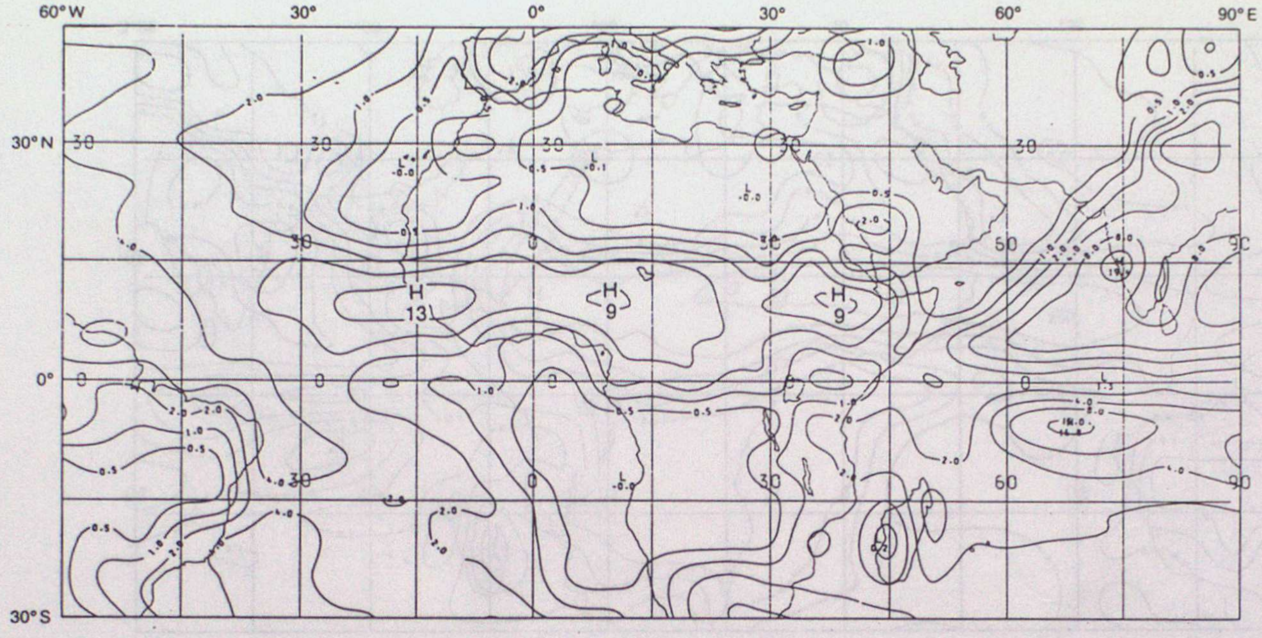

Figure 6 Modelled August rainfall for experiment 1984(I). Contours as in Fig. 4.

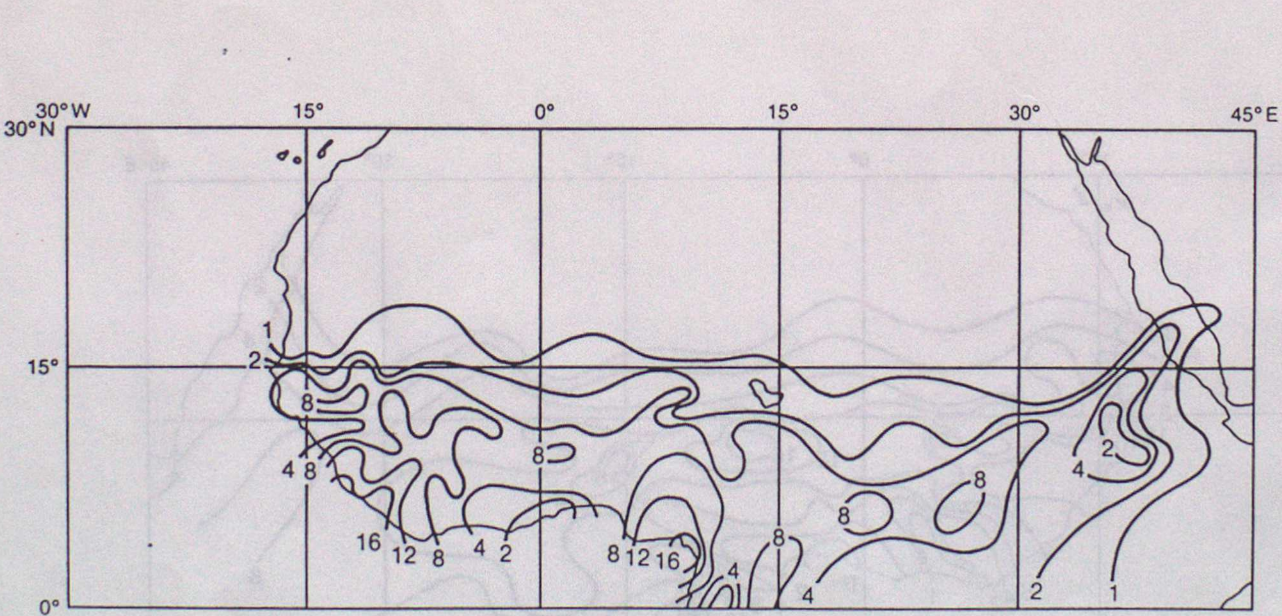

Figure 7 Observed rainfall for August 1984. Contours as in Fig. 5.

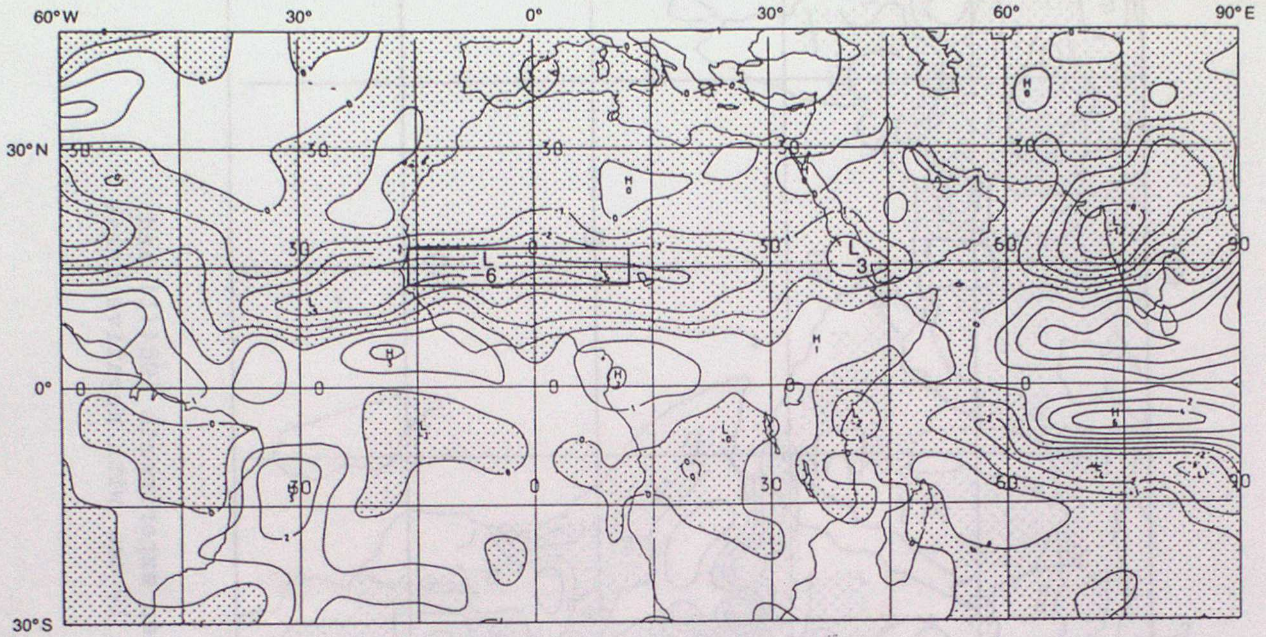

Figure 8 Modelled rainfall, difference between experiments 1984(I) and 1950(I) for July to September. Contours are at 0, ±1, 2, 4, 8, and 16 mm day⁻¹, with negative areas stippled.

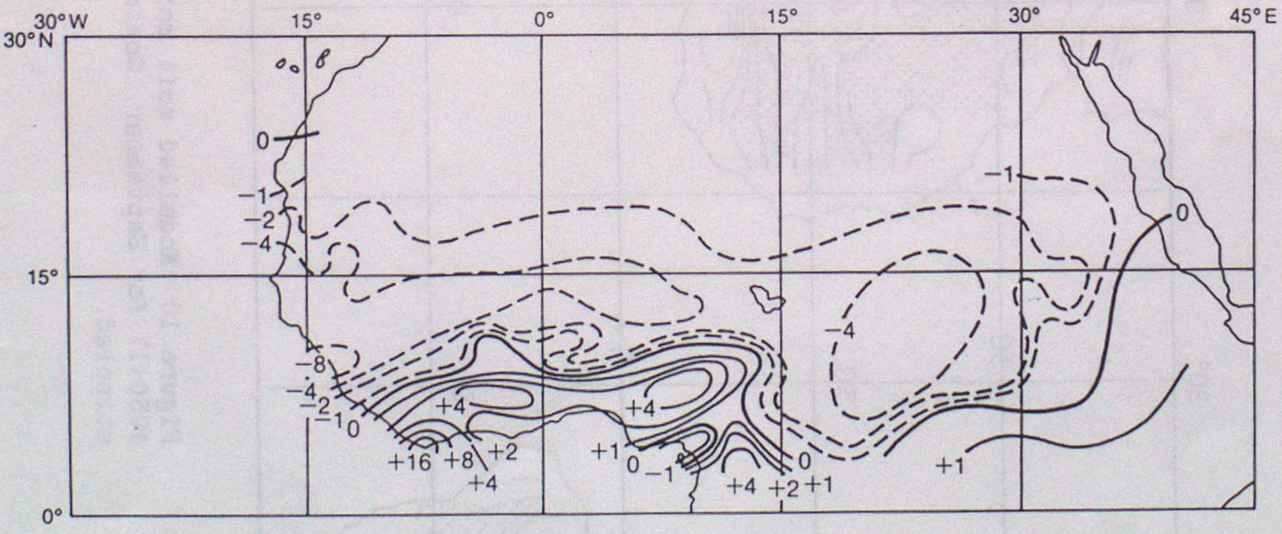

Figure 9 Observed rainfall, difference between 1984 and 1950 for July to September. Contours as in Fig. 8.

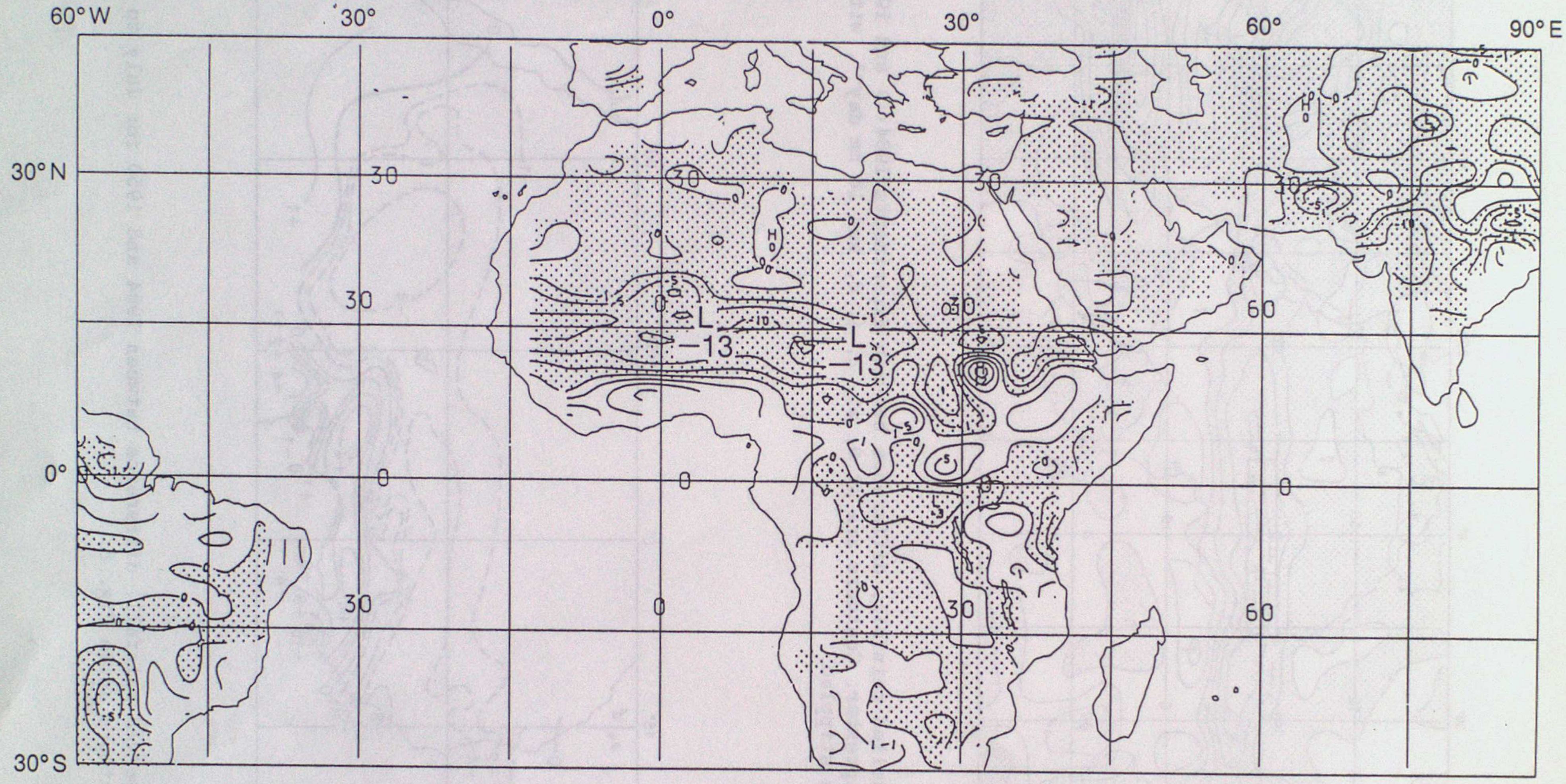

Figure 10 Modelled soil moisture, difference between experiments 1984(I) and 1950(I) for September. Contours are at 0, ±1, 5 and 10 cm, with negative areas stippled.

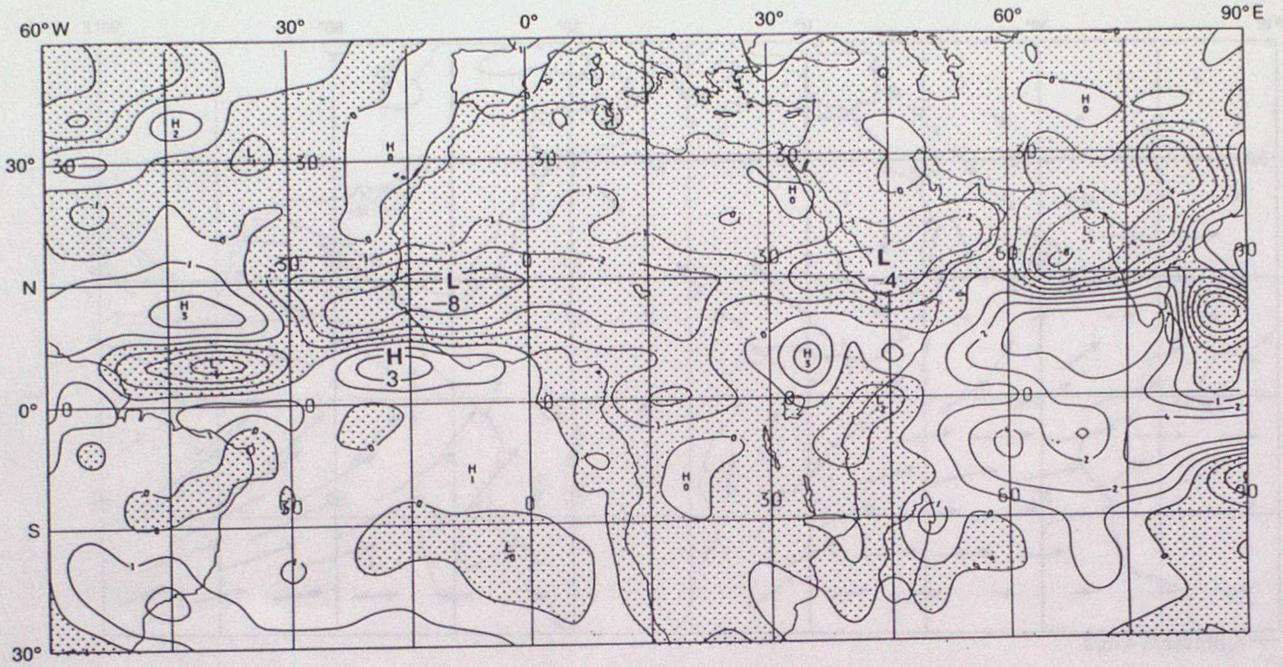

Figure 11 Modelled rainfall, difference between experiments 1983(I) and 1958(I) for July to September. Contours as in Fig. 8.

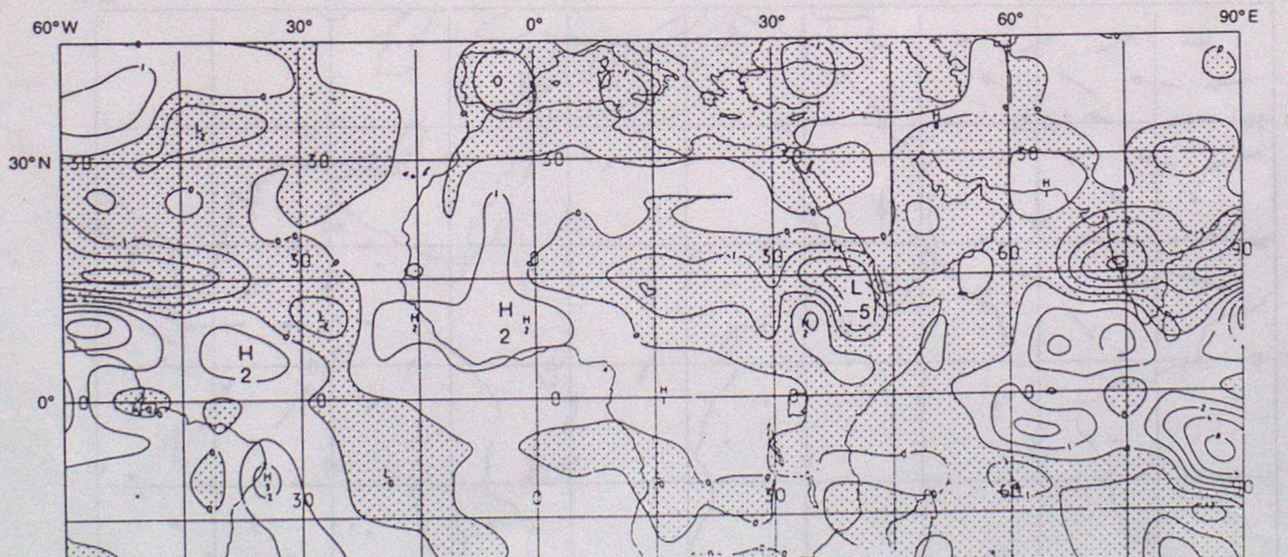

Figure 12 Modelled rainfall, difference between experiments 1984(I) and 1950(I) for July to September, but using model 4. Contours as in Fig. 8.

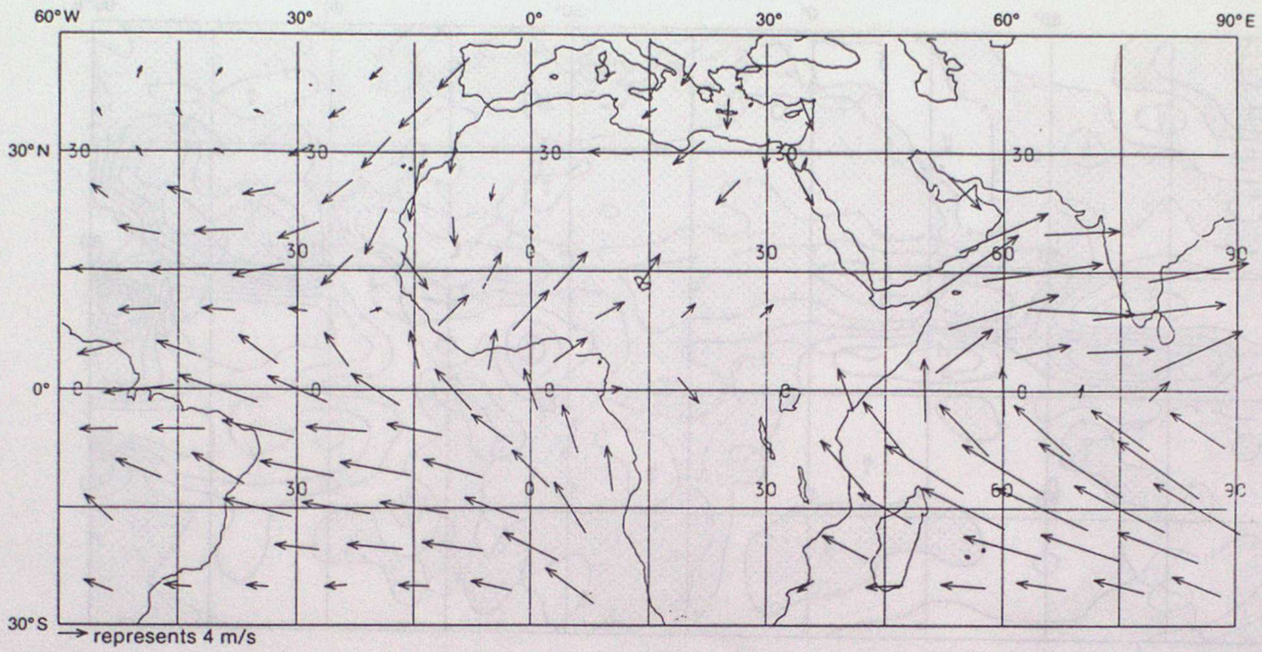

Figure 13 950 mb wind climatology for model 3 for July to September.

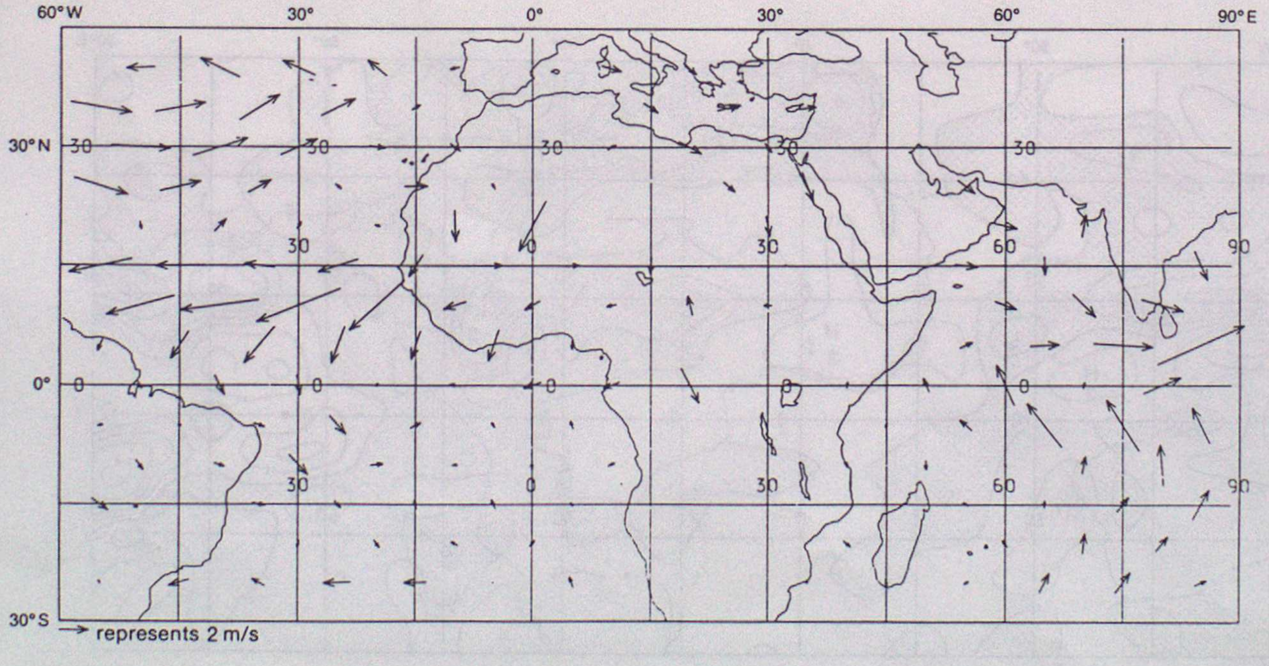

Figure 14 950 mb vector wind difference between experiments 1984(I) and 1950(I). Note change of wind scale from Fig. 12.

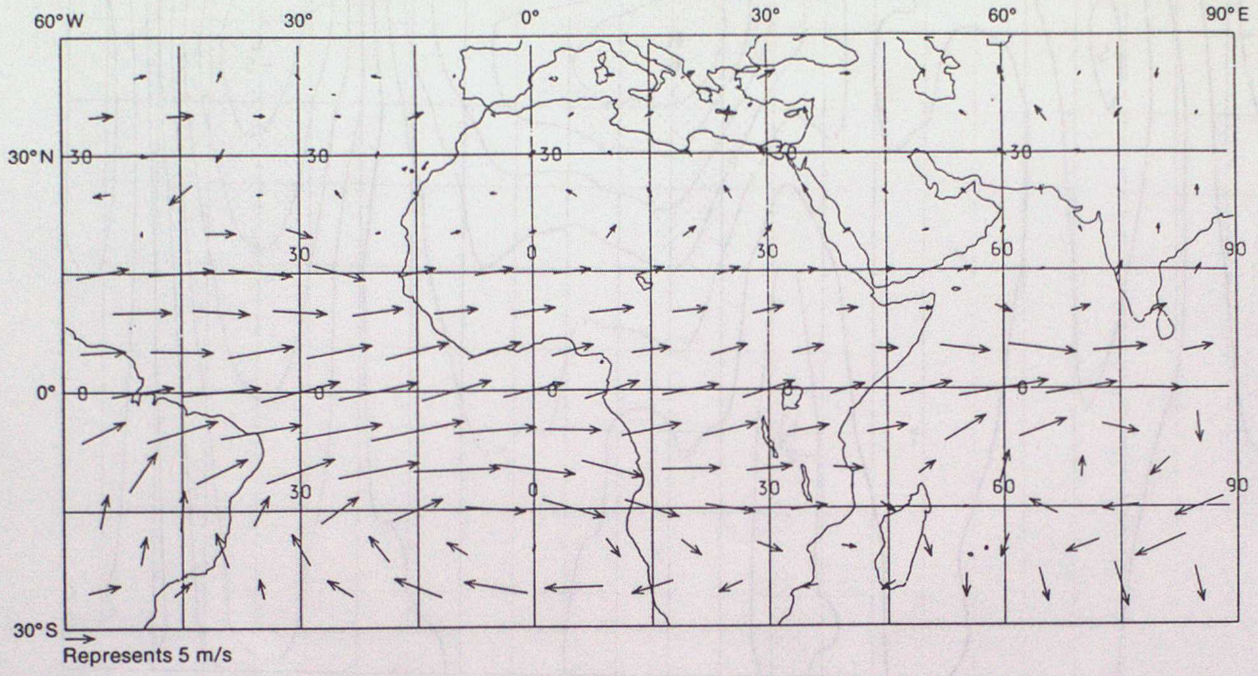

Figure 15 As Fig. 14 but for 250 mb wind.

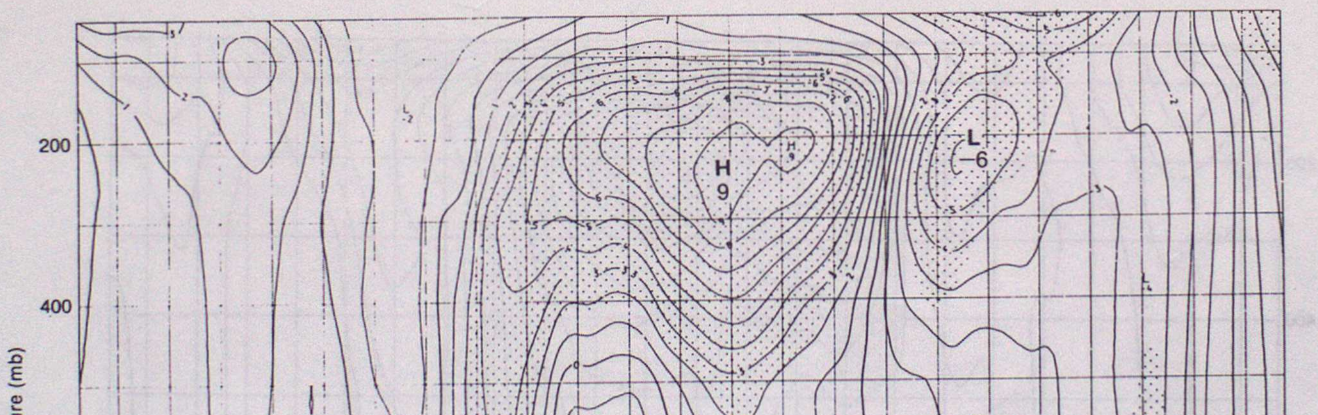

Figure 16 Cross-section (average over longitudes 10°W to 30°E) of the zonal wind difference between experiments 1984(I) and 1950(I) (combining the results from models 3 and 4) for July to October. Contour interval is 1 m s⁻¹. Areas where this difference is significant at the 95% confidence level are dotted.

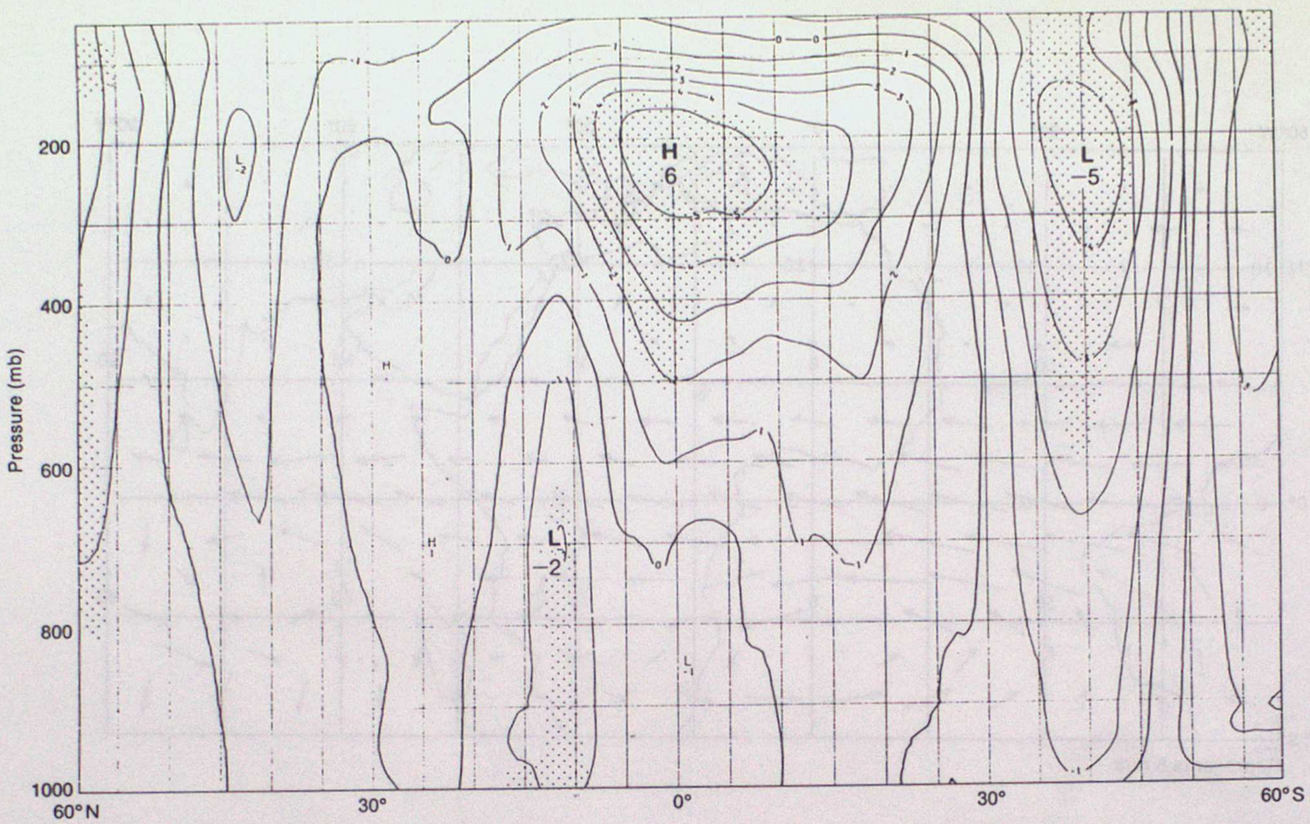

Figure 17 As Fig. 16, but for the difference between experiments 1983(I) and 1958(I) (using only the results from model 3).

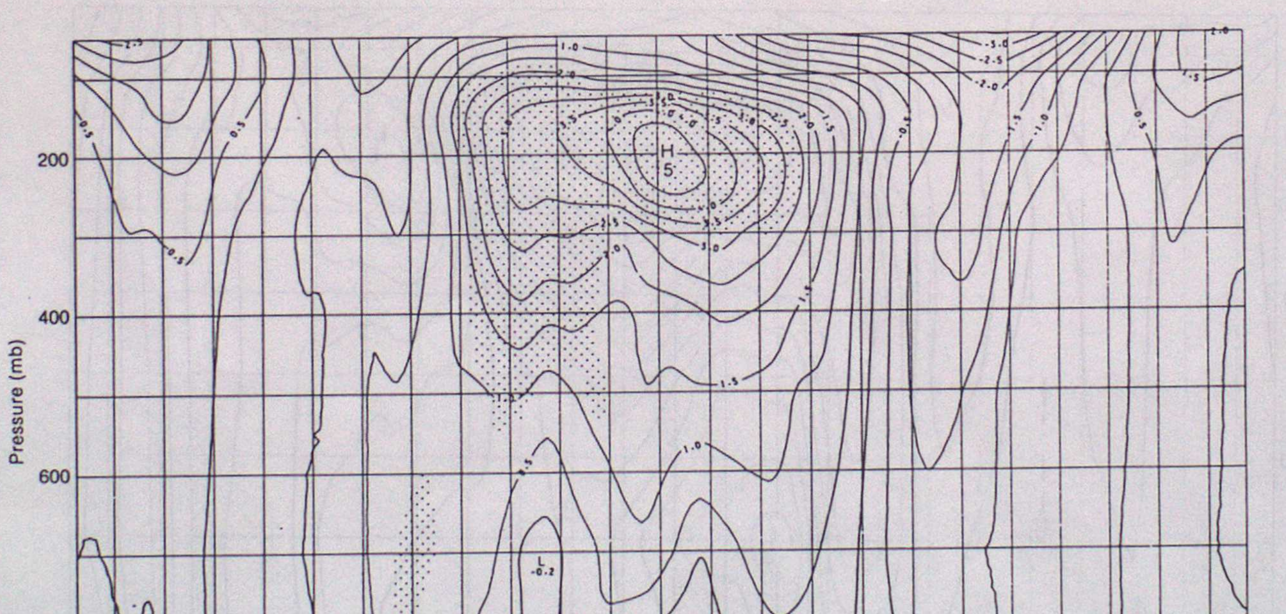

Figure 18 Cross-section (average over the whole globe) of the zonal wind difference between the average of experiments 1983(I) & 1984(I) and the average of experiments 1950(I) and 1958(I) for July to October (using only the results from model 3). Other details as in Fig. 16.

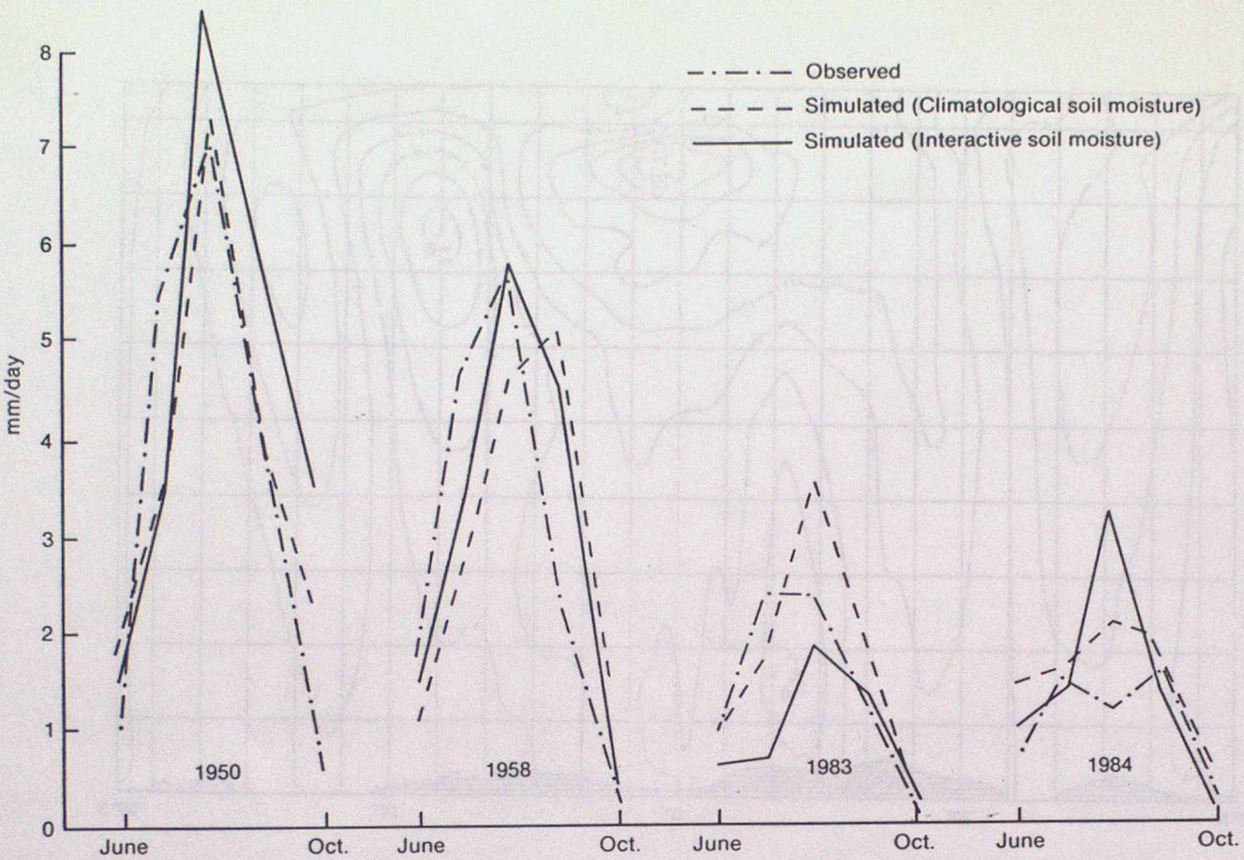

Figure 19 Time series of simulated rainfall for the whole Sahel for experiments 1950(I), 1958(I), 1983(I), 1984(I), 1950(C), 1958(C), 1983(C) and 1984(C), together with the corresponding observed rainfall.

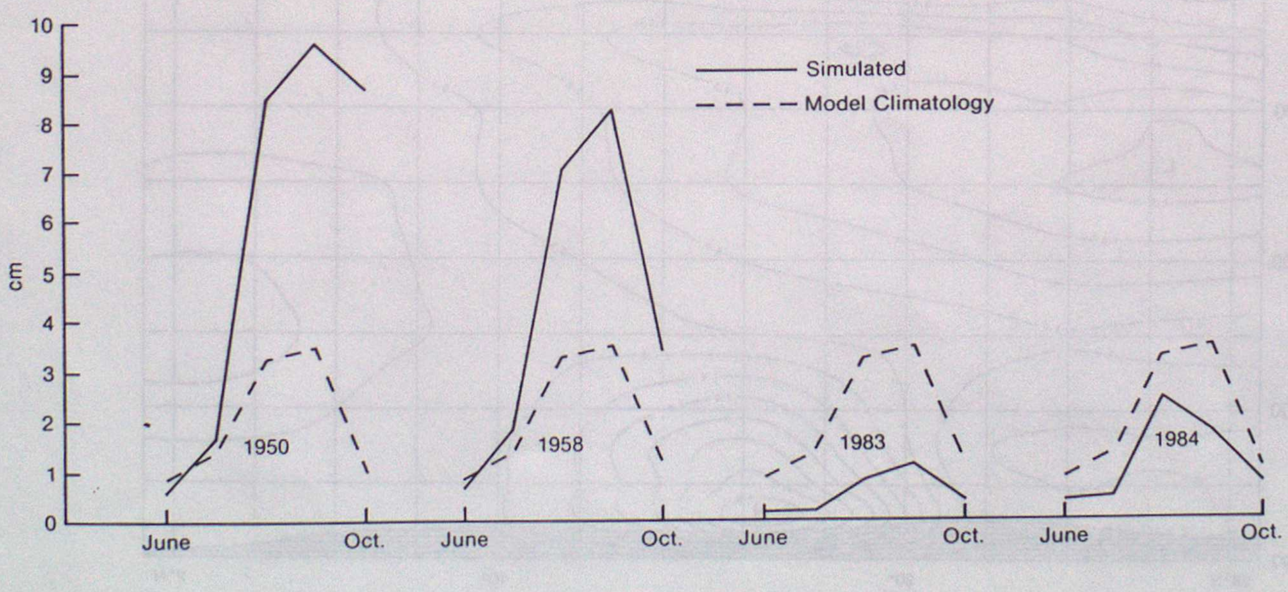

Figure 20 Time series of simulated soil moisture for the whole Sahel for experiments 1950(I), 1958(I), 1983(I) and 1984(I) together with the climatology of model 3.

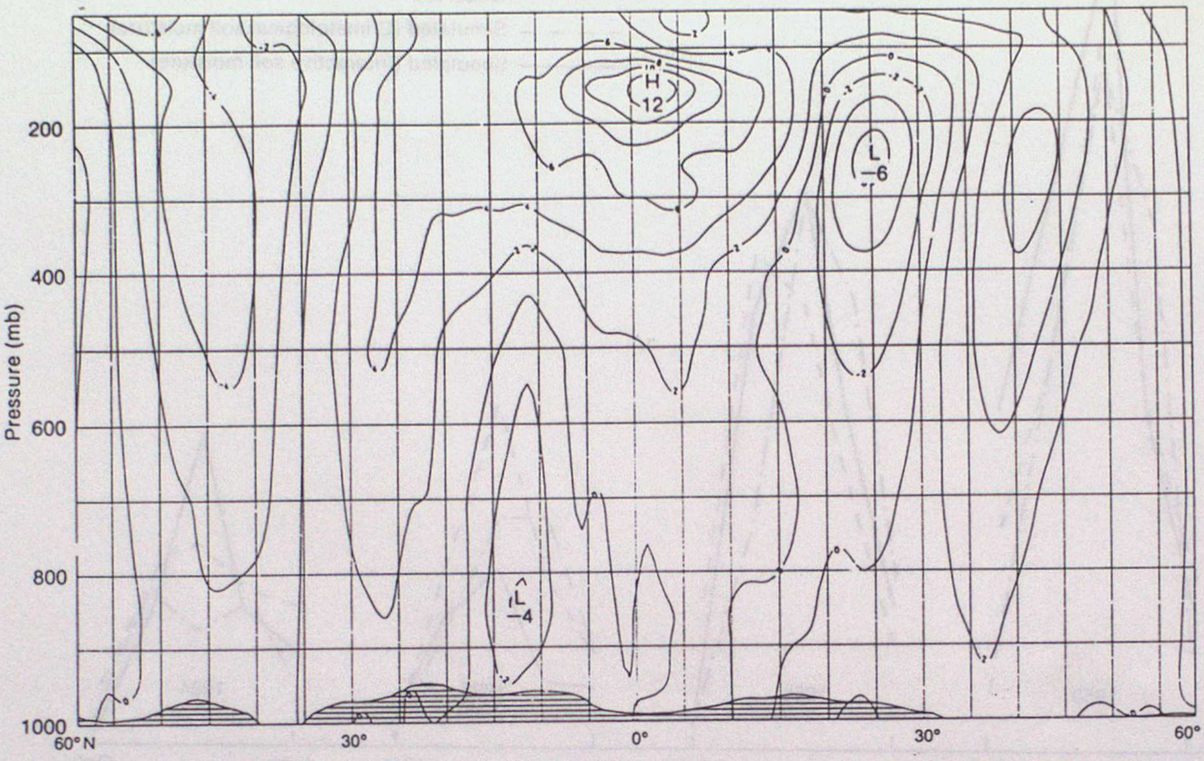

Figure 21 Cross-section (average over longitudes 10°W to 30°E) of the zonal wind difference between experiments 1984(C) and 1950(C) for July to September. Contour interval is 2 m s^{-1}.

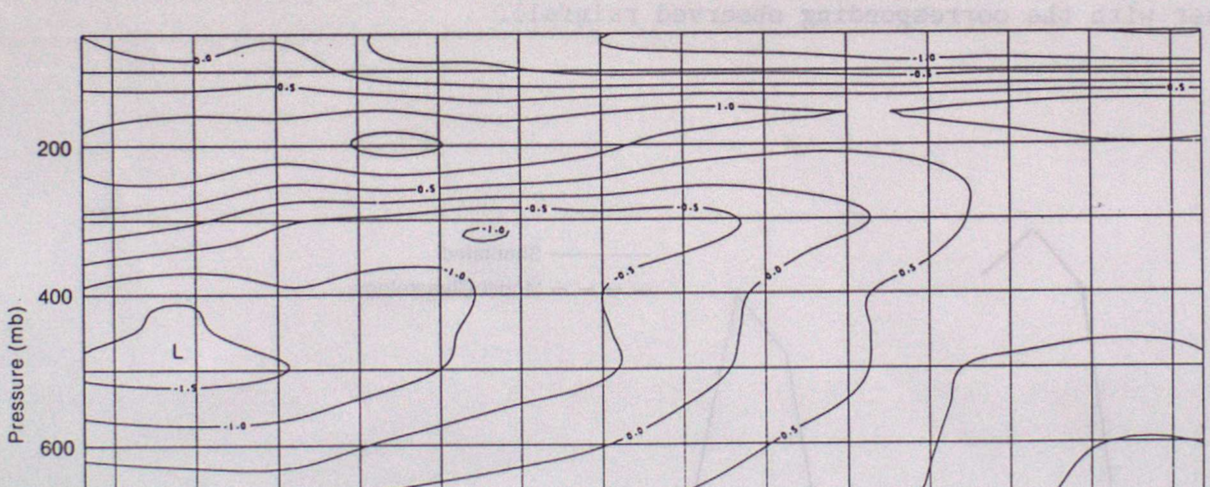

Figure 22 Cross-section (average over longitudes 10°W to 30°E) of the temperature difference between experiments 1984(I) and 1950(I) for July to September. Contour interval is 0.5 °C.

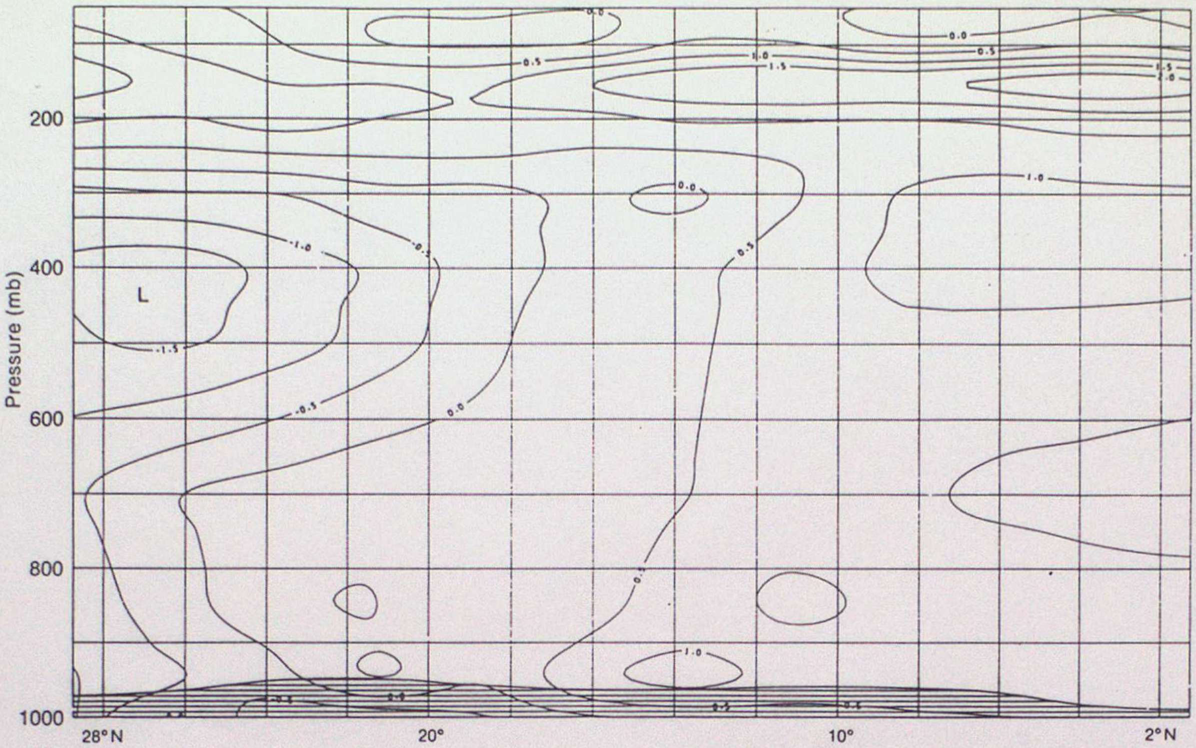

Figure 23 As Fig. 22 but for experiments 1984(C) and 1950(C).

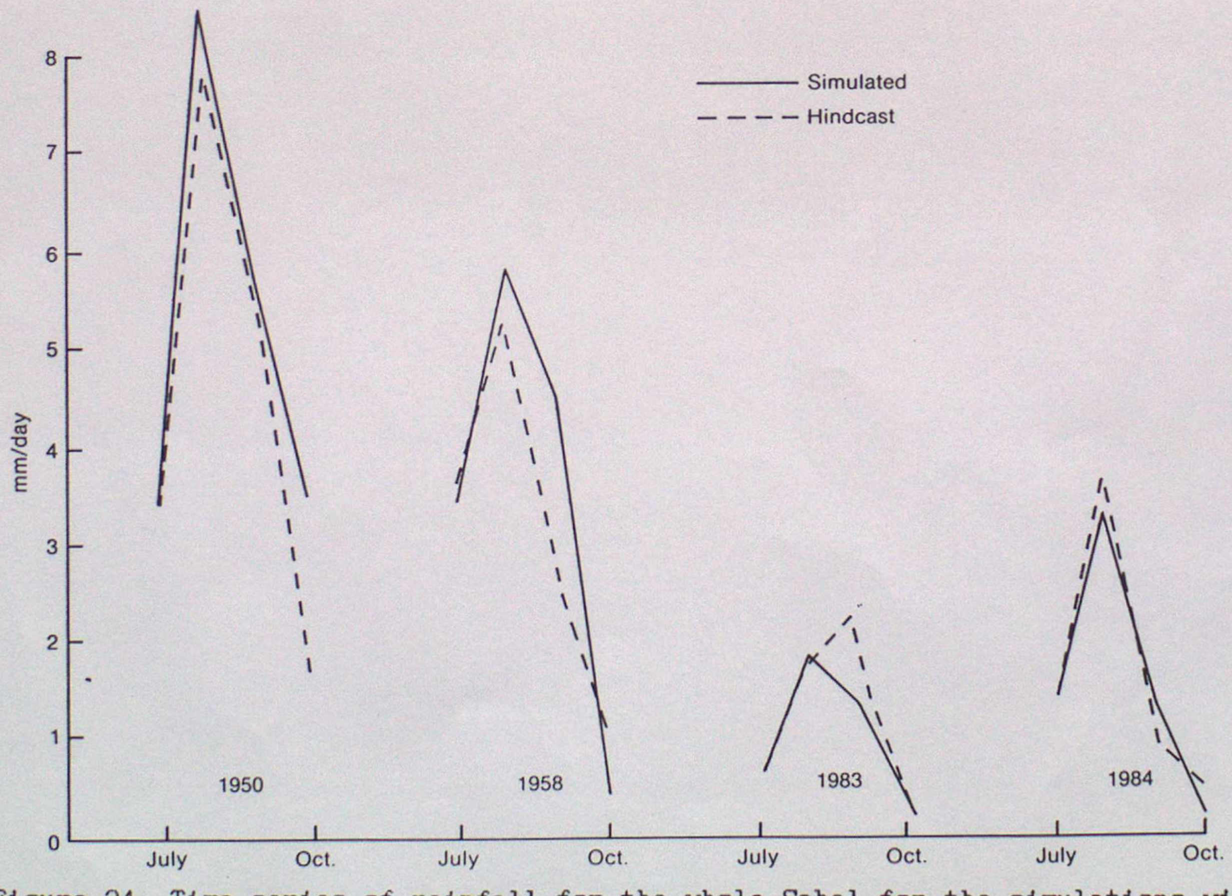

Figure 24 Time series of rainfall for the whole Sahel for the simulations with observed SSTs (1950(I), 1958(I), 1983(I) and 1984(I)) and the hindcasts with fixed SST anomalies (1950(F), 1958(F), 1983(F) and 1984(F)).

INDEX TO LONG-RANGE FORECASTING AND CLIMATE RESEARCH SERIES